Ecological Indicators 50 (2015) 79–89

Contents lists available at ScienceDirect

Ecological Indicators

journal homepage: www.elsevier.com/locate/ecolind

Simulation of watershed hydrology and stream water quality under land use and climate change scenarios in Teshio River watershed, northern Japan

Min Fan [a,*], Hideaki Shibata [b]

[a] Graduate School of Environmental Science, Hokkaido University, Kita 10, Nishi 5, Kita-ku, Sapporo 060-0810, Japan
[b] Field Science Center for Northern Biosphere, Hokkaido University, Kita 9, Nishi 9, Kita-ku, Sapporo 060-0809, Japan

ARTICLE INFO

Article history:
Received 12 December 2013
Received in revised form 30 October 2014
Accepted 3 November 2014

Keywords:
Water cycling
Sediment export
Nitrogen and phosphorous cycling
CLUE model
SWAT model

ABSTRACT

Quantitative prediction of environmental impacts of land-use and climate change scenarios in a watershed can serve as a basis for developing sound watershed management schemes. Water quantity and quality are key environmental indicators which are sensitive to various external perturbations. The aim of this study is to evaluate the impacts of land-use and climate changes on water quantity and quality at watershed scale and to understand relationships between hydrologic components and water quality at that scale under different climate and land-use scenarios. We developed an approach for modeling and examining impacts of land-use and climate change scenarios on the water and nutrient cycles. We used an empirical land-use change model (Conversion of Land Use and its Effects, CLUE) and a watershed hydrology and nutrient model (Soil and Water Assessment Tool, SWAT) for the Teshio River watershed in northern Hokkaido, Japan. Predicted future land-use change (from paddy field to farmland) under baseline climate conditions reduced loads of sediment, total nitrogen (N) and total phosphorous (P) from the watershed to the river. This was attributable to higher nutrient uptake by crops and less nutrient mineralization by microbes, reduced nutrient leaching from soil, and lower water yields on farmland. The climate changes (precipitation and temperature) were projected to have greater impact in increasing surface runoff, lateral flow, groundwater discharge and water yield than would land-use change. Surface runoff especially decreased in April and May and increased in March and September with rising temperature. Under the climate change scenarios, the sediment and nutrient loads increased during the snowmelt and rainy seasons, while N and P uptakes by crops increased during the period when fertilizer is normally applied (May through August). The sediment and nutrient loads also increased with increasing winter rainfall because of warming in that season. Organic nutrient mineralization and nutrient leaching increased as well under climate change scenarios. Therefore, we predicted annual water yield, sediment and nutrient loads to increase under climate change scenarios. The sediment and nutrient loads were mainly supplied from agricultural land under land use in each climate change scenario, suggesting that riparian zones and adequate fertilizer management would be a potential mitigation strategy for reducing these negative impacts of land-use and climate changes on water quality. The proposed approach provides a useful source of information for assessing the consequences of hydrology processes and water quality in future land-use and climate change scenarios.

1. Introduction

Land-use activities, which include conversion of natural landscapes for human use and changing management practices for human-dominated lands, have transformed a large proportion of the planet's land surface (Turner et al., 2001). Land-use change such as deforestation, increase and intensification of agricultural land, or expansion of urban land in a watershed can influence hydrologic processes, including infiltration, groundwater recharge, baseflow and runoff (Laurance, 2007; Lin et al., 2007; Bradshaw et al., 2007; Hurkmans et al., 2009). Watershed development from dominant natural land cover to more artificial land systems often reduces baseflow by changing groundwater flow pathways to surface water bodies (Lin et al., 2007). Croplands, pastures, plantations, and urban areas have expanded regionally and globally in recent decades, accompanied by large increases in

* Corresponding author. Tel.: +81 11 706 2587; fax: +81 11 706 3450.
E-mail address: firstfanmin@fsc.hokudai.ac.jp (M. Fan).

http://dx.doi.org/10.1016/j.ecolind.2014.11.003
1470-160X/

fertilizer application (Thampi et al., 2010; Tilman et al., 2001). Anthropogenic nutrient inputs to the biosphere from fertilizers now exceed natural nutrient sources, resulting in significant effects on water quality in streams, rivers, lakes and estuaries (Manson, 2005). Excessive fertilization of farmland often affects in-stream processes, such as biotic and abiotic immobilization and mineralization in river channels (Johnson et al., 1997). The major environmental consequences of excessive phosphorous and nitrogen inputs are water pollution, biodiversity loss, and eutrophication in aquatic ecosystems (Gitau et al., 2010; Chiang et al., 2010). Intensification of agricultural land including intensive cultivation of annual crops, plowing of soil on steep slopes, and poor soil conservation practices also produce serious soil erosion following soil nutrient depletion (Alibuyog et al., 2009). Fan and Shibata (2014a) reported that land use change (changing from paddy field to farmland field) remarkably impacted on hydrological and hydrochemical ecosystem services in the Teshio watershed, especially the nutrient retention was more sensitive to land use changes.

Global climate change, including changes of precipitation and temperature patterns, may significantly alter water quantity and quality in a watershed (USEPA, 2014). Global warming increases the water holding capacity of the atmosphere, resulting in global increases of precipitation and evapotranspiration (Howden et al., 2007). On average, global surface temperatures have increased about 0.74 °C over the past 100 years (Jeppesen et al., 2009). Winter temperature increase will cause more precipitation to fall as rain instead of snow, and snowpack will melt earlier in spring (Chiew and McMahon, 2002). Therefore, basin hydrology will shift from a combined rainfall/snowmelt regime to a more rainfall-dominant one, increasing flood risk in winter and the probability of droughts in summer. Higher temperature also increases potential evapotranspiration, which may lead to decreased runoff and soil moisture (Band et al., 1996; Stone et al., 2001; Jeppesen et al., 2009; Somura et al., 2009). Erosion and sediment transport processes are also influenced by climate change. For example, greater soil loss by erosion often occurs in regions with strong variability of precipitation and runoff (Marshall and Randhir, 2008). Moreover, soil erosion may cause significant offsite effects of river and reservoir sedimentation on hydroelectric power generation and irrigation efficiencies (Nelson et al., 2009). Murdoch et al. (2000) stated that a potential impact of climate change is increased diffusive sources of pollutant loads from agricultural land to river systems (Bouraoui et al., 2002). Increases of air and water temperature have been shown to increase biological productivity and decomposition, leading to an altered nutrient cycle, enhanced eutrophication, and degradation of water quality in a watershed (Chiew and McMahon, 2002; Jha et al., 2004; Bouraoui et al., 2004).

Fresh water is one of the most important resources for humans, flora and fauna (Bu et al., 2014). Terrestrial watershed and aquatic ecosystem provide bundles of ecosystem services such as water purification, provisioning of habitat for the aquatic organisms, flood control, water supply and food provision. As land use and climate changes and their effects become a pressing issue, it is important to understand the consequences it will have on water quantity and quality issues (Mander and Meyer, 2012). Human life and well-being depends on having clean water to use for drinking, food production, industrial uses, transportation and recreation, while ecosystems rely on clean water to provide life and habit. Rivers are open ecosystems which depend on their surrounding terrestrial landscape. The quantity and quality of river water could be dramatically affected by land use and climate changes and their negative consequence leads to decline in the services it provides. Nutrient export to running waters is conditional on landscape features like hydrology, climate, topography and soil types. The sediment and water quality are the critical environmental indicators to assess the water pollution degree and environmental health. The catchment-scale hydrochemical models could simulate the water quantity and quality under different land use and climate changes, which are useful for functional water management and land use planning to further sustain human benefits and the health of nature system (Pärn et al., 2012). Earlier studies have quantitatively assessed water quantity and quality under land-use or climate changes separately (e.g., Ferrier et al., 1995; Chang et al., 2001; Howden et al., 2007; Bradshaw et al., 2007; Metzger et al., 2008; Alibuyog et al., 2009; Fan and Shibata, 2014a). Few studies have analyzed and compared the impact of both land-use and climate changes on water quantity and quality, even though those changes are simultaneously occurred in the same period (Lin et al., 2007; Chiang et al., 2012). Therefore, modeling and understanding the responses of water quantity and quality to both land-use and climate changes in the future are very useful and valuable toward optimizing land-use planning, management and policy in a watershed, particularly one with expanding agriculture. Given this backdrop, this study uses model to assess the impacts of multiple land-use and climate change scenarios on hydrologic components and water quality at watershed scale. Specific objectives are: (1) to evaluate impacts of land-use and climate changes on water quantity and quality at watershed scale; (2) to analyze relationships between hydrologic components and water quality under different land-use and climate change scenarios at watershed scale. Our hypotheses were: (1) there are significant impacts of land-use and climate changes on water quantity and quality; (2) there are close relationships between hydrologic components and water quality under land-use and climate changes.

2. Methods

2.1. Overview of study approach

The overall analytical framework consists of land-use change modeling, development of climate change scenarios, and modeling of water, nutrient and sediment dynamics in a watershed. We simulated future land-use patterns using the Conversion of Land Use and its Effects (CLUE) model, which is based on logistic regression models and has driving factors including spatial policies and land-use demand. We developed the multiple climate change scenarios generated by a general circulation model (GCM) for the study watershed. Following the development of change scenarios for land use and climate, we applied the Soil Water and assessment Tool (SWAT) to simulate water, nitrogen, phosphorus, and sediment dynamics under multiple land-use and climate change scenarios at the watershed scale. We then analyzed relationships between hydrologic and water quality components to test the hypothesis that future land-use and climate changes will impact yields of water, sediment, nitrogen, and phosphorus in the watershed.

2.2. Study site

The study site is in the Teshio River catchment in northern Hokkaido of North Japan. The Teshio is the fourth longest river in Japan; it originates from the foot of Mt. Teshio and flows into the Sea of Japan (Ileva et al., 2009,b; Fan and Shibata, 2014a,b). The Teshio is a representative watershed of northern Japan. It consists of forest, agricultural land and human settlements, with average population ~90,000 concentrated in the middle and upper parts of watershed, which are dominated by agriculture (Fan and Shibata, 2014a). Ileva et al. (2009) stated that excess fertilizer application on agricultural land in the middle Teshio watershed increased

nitrate concentration in water of the river main channel and tributaries. This suggested that further transition of land use with climate change in the future would further affect water quality in this watershed. Fan and Shibata (2014a) indicated that spatial topography and temporal land-use changes strongly affected water yield and nutrient retentions in the Teshio watershed. The alteration of water quality and quantity also impacts environmental quality downstream and in estuaries those are important habitats for aquatic biota (Ileva et al., 2009). In this study, we focused on the upper and middle Teshio watershed (Fig. 1), where urban and agricultural lands are mostly located. The catchment area of the study site is 2908 km^2. Average water flow is 138.6 $m^3 s^{-1}$, with the maximum 1278 $m^3 s^{-1}$ in April during snowmelt and the minimum 19.8 $m^3 s^{-1}$ is in midwinter (February) at Bifuka monitoring station (Fig. 1). Approximately 78% of land in the catchment is covered by cool-temperate mixed forest, including deciduous broadleaved and evergreen coniferous species with a dense understory of *Sasa* dwarf bamboo (Ileva et al., 2009; Fan and Shibata 2014a). Other land uses are mainly farmland and paddy fields, with percentage coverage 13% and 4%, respectively. Farmland in the watershed is mainly used for upland crops such as potato, pumpkin, wheat, maize, asparagus, and others. The farmland and paddy fields concentrate in the both sides of the river and the southwestern watershed. Soil is predominately brown forest soil (Cambisol; IUSS Working Group WRB, 2006). Others are gray lowland soil (Gleyic Fluvisols; IUSS Working Group WRB, 2006), brown lowland soil (Haplic Fluvisols; IUSS Working Group WRB, 2006), gray soil (Gleyic Fluvisols; IUSS Working Group WRB, 2006), and peat soil (Histosols; IUSS Working Group WRB, 2006).

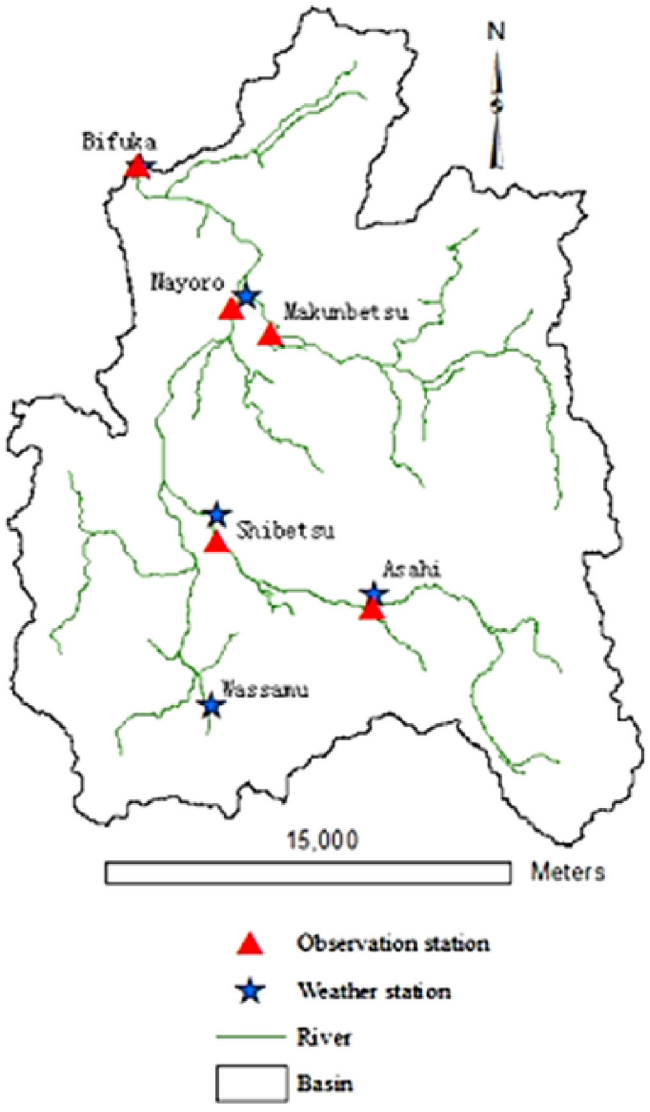

Fig. 1. Upstream of Teshio watershed.

2.3. Land-use change model

We predicted future land-use patterns in the watershed according to the current temporal trends of land-use transition from past to present using the CLUE model. In the CLUE model, the non-spatial module calculates the area of change for all land-use types at an aggregate level, and the spatial module translates demands into land-use change at various locations within the study region (Verburg and Overmars, 2009). Relationships between land use and its drivers can be fit using stepwise logistic regression established by Fan and Shibata (2014a) in this watershed. Furthermore, probability maps for all land-use types were established using logistic regression models. Relationships between land use and its drivers were evaluated by the following stepwise logistic regression:

$$\mathrm{Log}\left(\frac{P_i}{1-P_i}\right) = \beta_0 + \beta_1 X_{1,i} + \beta_2 X_{2,i} + \cdots + \beta_n X_{n,i} \quad (1)$$

where P_i denotes the occurrence probability at a grid cell of a given land-use type. $X_{1,i} \cdots X_{n,i}$ are driving factors, and $\beta_0 \cdots \beta_n$ are coefficients of each driving factor in the logistic model.

We did not define in the simulation any conservation area for future land use. In the CLUE model, topography and soil characteristics are dealt with by driving factors to form the spatial pattern of land use. Topographic and soil parameters included soil type, elevation, slope, aspect, and distances to water bodies, roads and urban areas for the logistic analysis (Millington et al., 2007). We applied those parameters using a publicly available database (National Land Information Office of the Ministry of Land, Infrastructure, Transport and Tourism or MLIT; http://nlftp.mlit.go.jp/ksj-e/). The aptitude of the model was evaluated with the Receiver Operating Characteristic (ROC) method, which determines predicted probabilities by comparing them with observed values over the entire domain of those probabilities. If the ROC value approximates one, then the model prediction is considered to approach perfection (Pontius and Schneider, 2000). Land-use datasets from 1976 and 2006 were also obtained from the National Land Information Office of MLIT. In the study watershed, there were eight land-use types: paddy field, farmland, forest, pasture, urban, road, factory, and water body. We simulated future land use in 2036 according to variation trend of land-use change between 1976 and 2006, using the CLUE model (Fan and Shibata, 2014a).

2.4. Climate change scenarios

Observed climate datasets of precipitation and temperature for 24 years (1976–2009) were used as the baseline climate scenario. We used GCM prediction model to simulate future climate during 2010–2039 (hereafter called short-term change), 2040–2069 (mid-term change) and 2070–2099 (long-term change). First, the future climate change scenarios were derived from the Model for Interdisciplinary Research on Climate (MIROC) model (MIROC3.2-HI) under the Special Report on emissions scenarios B1 (SRB1) scenario of Intergovernmental Panel on Climate Change (IPCC, 2007). The scenario used for the model was created using

warming predictions by Center for Climate System Research/National Institute for Environmental Studies (CCSR/NIES) for modifying regional historical precipitation and temperature observations (IPCC, 2007). The SRB1 includes improved emission baselines and the latest information on economic restrictions throughout the world. SRB1 examines different rates and trends of technological change and expands the range of various economic development pathways, including narrowing of the income gap between developed and developing countries (IPCC, 2007). All modeled data for MIROC3.2-HI was obtained from the Data Distribution Centre of IPCC. Since spatial resolutions of GCMs are too coarse to represent local climate characteristics in our watershed, simple downscaling between the baseline and climate scenario of the nearest GCM grid was applied directly. Future change of temperature in the study area was assumed equal to the difference between temperatures simulated using GCMs for future and current conditions at a weather station in the watershed. Thus, future change of temperature was estimated as follows (Tung et al., 2005).

$$\mu\prime_{mT} = \mu_{mT} + (\mu_{mT,\text{future}} - \mu_{mT,\text{current}}) \quad (2)$$

here, μ_{mT} and μ'_{mT} are current and future mean monthly temperatures (°C), respectively; $\mu_{mT,\text{current}}$ and $\mu_{mT,\text{future}}$ are simulated mean monthly temperature under the current and future scenario climate conditions, respectively. Future change of precipitation was assumed to be the ratio of precipitation in the future condition to that in the current condition (Tung et al., 2005):

$$\mu\prime_{mP} = \mu_{mP'}\left(\frac{\mu_{mP,\text{future}}}{\mu_{mP,\text{current}}}\right) \quad (3)$$

here, μ_{mP} and μ'_{mP} are the current and future mean monthly precipitation, respectively. $\mu_{mP,\text{curent}}$ and $\mu_{mP,\text{future}}$ are simulated mean monthly precipitation under the current and future scenario climate conditions, respectively. Climate changes estimated based on the IPCC-DCC Fourth Assessment Report SRB1 scenario (IPCC, 2007) for the study site are given in Table 1. According to the above procedures, we calculated average data for short-term, mid-term and long-term climate changes for the following model simulation. The generation method of daily climate data for that simulation is described in the next section.

2.5. Hydrology and water quality model

The SWAT is a hydrology and water quality model developed by the United States Department of Agriculture Agricultural Research Service (Arnold and Allen, 1996). In this model, the watershed is divided into multiple sub-watersheds, which are then divided into units of unique soil, land-use and slope characteristics called hydrologic response units (HRUs). In the SWAT, water, sediment and nutrient transformations and losses determined in each HRU are aggregated at the sub-basin level and routed to the catchment outlet through the channel network. The hydrologic sub-model is based on the water balance equation in the soil profile, where the simulated processes include precipitation, infiltration, surface runoff, evapotranspiration, lateral flow, and percolation (Fan and Shibata, 2014b). The sediment yield sub-model is based on the modified soil loss equation developed by Williams and Berndt (1977). The nutrient cycle sub-model was developed based on single growth model as a part of the Environmental Policy Integrated Climate (EPIC) model which is used for simulating all plants (Williams et al., 1984). In this sub-model, plant phenological processes of the crop are driven by daily heat unit accumulation. Plant growth can be inhibited by temperature, water or nutrient stress. Plant growth is modeled by simulating leaf area development, light interception and conversion of intercepted light into biomass assuming plant species-specific radiation-use efficiency. Plant nutrient uptake is controlled by the plant nutrient equation which determines the fraction of nitrogen in the plant biomass as a function of growth stage given growing conditions. The EPIC simulates movement and transformation of nitrogen (N) and phosphorous (P) in the catchment, such as mineralization of organic N and P, denitrification, volatilization, plant nutrient uptake, microbial immobilization of N and P and their leaching from soil to groundwater and river.

The SWAT model requires meteorological data such as daily precipitation, maximum and minimum air temperature, wind speed, relative humidity, and solar radiation. We used Sharpley and Williams's WXGEN weather generator within the SWAT to generate daily temperature and precipitation data for the target climate scenarios (Sharpley and Williams, 1990). To obtain statistical weather parameters of stochastic processes and distributions in WXGEN (Williams and Griffiths, 1995; Neitsch et al., 2011), we used observed climate data from 1997 to 2009, because continuous daily data for precipitation and temperature were available for this period.

Another requirement of spatial input data for SWAT is a digital elevation model (DEM) and maps of land-use and soil type (described in Section 2.3). The SWAT also requires data on N and P fertilizer input to agricultural land and atmospheric N deposition to the entire watershed. We used data of Mishima et al. (2010) on past N and P fertilizer input in 1985, under 1976 land use. Fertilizer input

Table 1
Changes of temperature and ratios of precipitation predicted by MIROC3.2-HI models, based on SRB1 scenarios.

Month	Station		MIROC3.2-HI (44.27°E, 142.88°N)					
	T (°C)	P (cm)	ΔT (°C)			Ratio (cm cm^{-1})		
	Baseline scenario		Short-term (2010-39)	Mid-term (2040-69)	Long-term (2070-99)	Short-term (2010-39)	Mid-term (2040-69)	Long-term (2070-99)
1	−9.20	0.87	1.70	3.30	4.20	1.01	1.03	1.17
2	−8.90	0.62	2.00	3.20	4.00	1.11	1.02	1.20
3	−3.50	0.61	1.80	3.50	4.20	1.10	1.29	1.24
4	3.70	0.50	2.50	4.40	4.90	1.10	1.09	1.16
5	10.30	0.59	1.60	2.60	3.30	0.89	0.90	0.98
6	15.10	0.60	1.60	2.60	3.30	1.13	1.13	1.23
7	19.00	1.08	1.50	3.00	4.20	0.98	1.02	1.27
8	20.20	1.26	1.90	2.80	3.50	1.06	1.21	1.18
9	14.90	1.35	1.60	2.50	3.30	1.10	1.23	1.39
10	8.20	1.36	1.80	3.00	3.70	0.93	0.92	0.82
11	1.20	1.44	1.80	3.00	4.10	1.10	1.05	1.05
12	−5.30	1.20	1.70	2.70	3.90	1.11	1.17	1.17
Average	5.50	0.96	1.79	3.05	3.88	1.05	1.09	1.16

data of N and P in 2005 (also by Mishima et al., 2010) was used as those under 2006 and 2036 land-use scenarios. The detailed information on timing and amount of fertilizer for different crops is in the Table A-1. We assumed that the manure fertilizers were applied in May and chemical fertilizers were used in June and August. Those schedules of fertilizer application were arranged to fit the model with the observed water quality in the calibration and validation of the SWAT model. Because the potato is a representative crop in farmland of the study watershed, we used the potato parameter for farmland crops in the entire SWAT simulation.

Atmospheric N deposition data within the study watershed was unavailable. Therefore, we used N concentration data for atmospheric deposition, observed at the nearest long-term monitoring site, in the Uryu Experimental Forest (at Moshiri in Horokanai town, N44°21.7′, E142°15.9′, ~20 km west of the city of Nayoro; Fig. 1). This is a core site of the Japan Long-Term Ecological Research Network (Noguchi et al., 2010; database for acid deposition of Japan at http://db.cger.nies.go.jp/dataset/acidrain/).

First, the SWAT model was directly set up for streamflow, sediment, N and P loads of 2001–2002, 2003–2007 and 2008–2009
as warm-up, calibration, and validation periods, respectively. We used observed data of water discharge and loads of sediment, total N and P in river water at Bifuka monitoring station (Fig. 1) for model validation (http://www1.river.go.jp/). Observed mean annual yields of water, sediment, total N and P during 2001–2009 were 435.2–697.1 mm year^{-1}, 0.045–0.074 Mg ha^{-1} year^{-1}, 4.33–9.65 kg N ha^{-1} year^{-1} and 0.24–0.36 kg P ha^{-1} year^{-1}, respectively. Model performance was evaluated by the coefficient of determination (R^2) and Nash–Sutcliffe simulation efficiency (NSE) (Nash and Sutcliffe, 1970).

3. Results

3.1. Land-use change model predictions

In land-use simulation of the CLUE model, ROC values of the logistic regression model were greater than 0.7, indicating an adequate fit for simulating land-use change based on land-use demand areas (Annex, Tables A-2 and A-3). Fig. 2 shows that forest occupied about 70% of the entire watershed and was dominant in all three periods (1976, 2006 and 2036). Paddy and farmland was mostly in flat and riverine areas. The area of paddy field decreased from 1976 to 2036, while that of farmland increased. In conclusion, agricultural land became more farmland-dominated with a decrease of paddy fields in future land use. Most paddy field area and some forest and pasture would change to farmland for satisfying agricultural expansion in the study watershed. Those simulations of land-use changes in the Teshio watershed were also reported in Fan and Shibata (2014a).

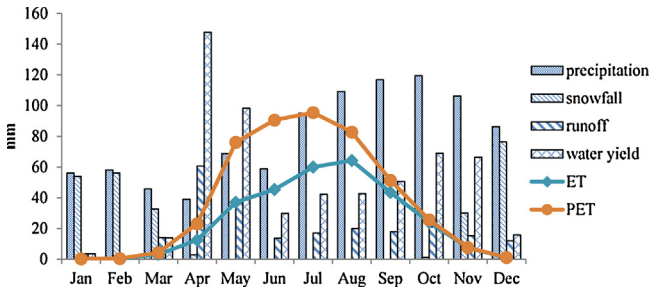

Fig. 3. Average monthly precipitation, snowfall, runoff, water yield, evapotranspiration and potential evapotranspiration under baseline climate conditions and 2006 land use.

3.2. Seasonal change of water balance components under baseline climate conditions with 2006 land use

For calibration and validation of the SWAT model, NSE and R^2 values for streamflow, sediment, and total N and P were greater than 0.5, which indicate a satisfactory model. Fig. 3 presents seasonal change of hydrologic components under 2006 land use and the baseline climate. Annual average precipitation during the study period was 959 mm, with highest values in October as rainfall. An average 252 mm snowfall occurred from October through April. Average snowfall began in October and increased to a maximum in February, decreasing in April. Annual surface runoff averaged 234 mm, with maxima in April and May from spring snowmelt (Fig. 3). The lowest runoff rates were in January and February, when snowpack was deepest and temperature the coldest. The SWAT predicted water yield within the watershed, including groundwater yield and surface runoff flows. Potential evapotranspiration (PET) in the watershed averaged 459 mm year^{-1}, with the highest value in July (Fig. 3). The highest actual evapotranspiration (ET) was simulated for July and August, with the greatest difference between PET and ET in June and July. Average ET from May through August was 34.5 mm month^{-1}, less than the PET (Fig. 3). Details of spatial distribution and seasonal changes of hydrological process in Teshio watershed are also found in Fan and Shibata (2014b).

3.3. Seasonal change in water balance components under multiple climate change scenarios and 2006 land use

Based on climate scenarios, annual average precipitation increased from 958.7 mm under the baseline climate to 1099 mm

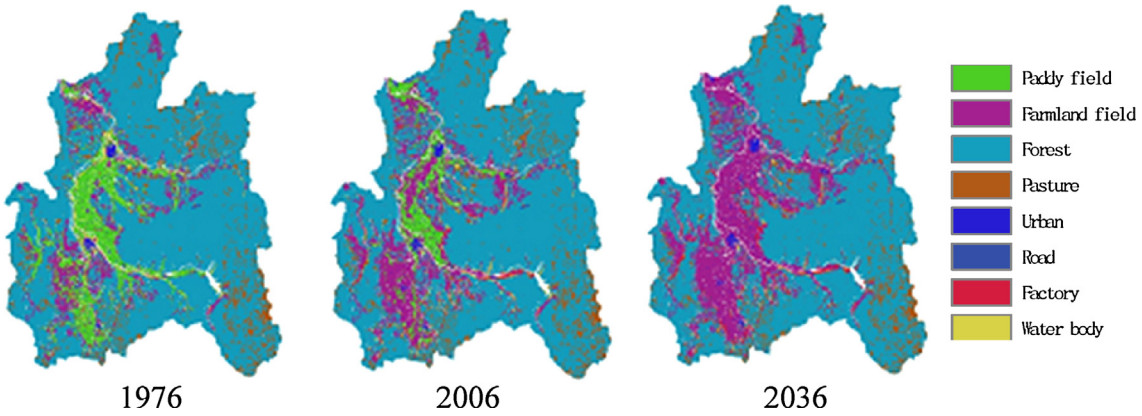

Fig. 2. Land-use map of 2036 from the CLUE model, based on land-use maps for 1976 and 2006.

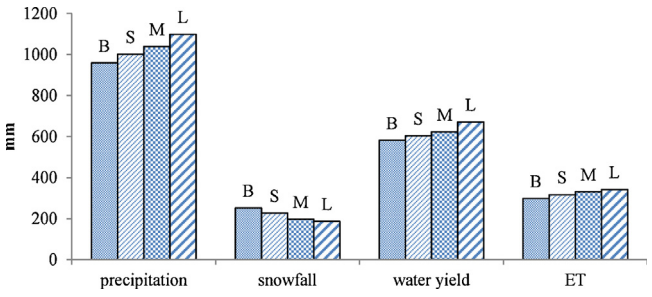

Fig. 4. Annual average precipitation, snowfall, water yield and evapotranspiration under climate change scenarios and 2006 land use. B, S, M and L in the scenarios mean climate changes in baseline (observed for 1976–2009), short-term prediction (2010–2039), mid-term prediction (2040–2069) and long-term prediction (2070–2099), respectively.

with long-term climate change (Fig. 4). There was a marked reduction of annual snowfall under a warmer climate (Fig. 4), owing to the temperature increase during winter (Table 1). All climate change scenarios caused greater monthly precipitation than that of the baseline climate, especially in September, but May and October had different tendencies (Fig. 5a). In October, all climate change scenarios reduced monthly precipitation over that of the baseline climate. The maximum reduction in snowfall was from October through April for the long-term climate change scenario (Fig. 5b), in which average temperature increased by 3.88 °C (Table 1). Snowfall decreased in November, December and March for all scenarios. Snowfall in October and April decreased to zero in the mid-term and long-term scenarios, and changes of snowfall in January and February were not apparent (Fig. 5b). In other words, the snow-cover-free period increased from 5 months (May through September) under baseline climate to 7 months (April through October) under future climate change conditions (Figs. 3 and 5b). Monthly average surface runoff increased under three climate change scenarios in January, February, March, August, September, November and December, with the peak value in March (Fig. 5c). Monthly average surface runoff decreased under all scenarios in April and May (Fig. 5c). Changes of monthly average surface runoff in other months were not apparent (Fig. 5c). As expected, PET and ET increased under climate change scenarios, especially during snowmelt season (March and April) and summer (June and July) (Fig. 5d). Since ET was restricted by soil water availability, it was less than PET, especially from April through August (Fig. 5d). PET was estimated at 1.2 times greater than ET in March and April under the baseline climate. Under the long-term climate change scenario (3.88 °C increase of air temperature), PET doubled ET in March and April (Fig. 5d). Despite changes in the seasonal distribution of ET, the change of annual average ET was relatively small. The peak water yield was in April under the baseline climate and the short- and mid-term climate changes (Fig. 5e). Under the long-term change, the water yield maximum was in March, earlier than in other scenarios. Monthly water yields increased under all scenarios in January, February, March, September and December, whereas changes in other months were not apparent (Fig. 5e). Seasonal changes of water balance components were also predicted under all scenarios with 2036 land use (Annex, Fig. A-1).

3.4. Water quantity and quality under multiple changes of land-use and climate

Annual average surface runoff, lateral flow, groundwater, ET, and water yield varied with land use and multiple climate conditions (Table 2). All the hydrologic components in Table 2 were increased by climate change relative to the baseline climate for each land use (i.e., long-term > mid-term > short-term > baseline). Water yield under long-term climate changes for 2006 and 2036 land uses were 1.15 and 1.16 times higher than those under the baseline, respectively (Table 2). As a whole, annual change of hydrologic components from land-use changes of 1976, 2006 and 2036 were smaller than those for multiple climate changes (Table 2).

Under baseline climate conditions, annual sediment yield with 2006 land use was greatest among the three land uses, followed by 1976 and 2036 (Table 3). Climate change increased sediment yields for each land use (2006 and 2036). As a result, the highest sediment yield was under long-term climate change scenarios for 2006 land use (Table 3).

For all climate change scenarios, inorganic N was the generally dominant form of total N, whereas organic P was mostly dominant within total P (Table 3). Under the baseline climate scenario, total N and P yields for 1976 land use were the greatest, followed by those for 2006 and 2036 (i.e., 1976 > 2006 > 2036). Longer climate changes tended to increase both yields for each land use (i.e., long-term > mid-term > short-term > baseline climate). The variations of both yields by climate change were larger than those by land-use change (Table 3).

Tables 4 and 5 show fertilizer input, atmospheric N deposition, nutrient uptake by crops, denitrification, leaching, and mineralization of organic N and P predicted by the SWAT model. Fertilizer N and P were highest in 1976, followed by 2036 and 2006. Internal cycling of N and P, such as nutrient uptake and mineralization, was generally greater than their leaching. Under the 2006 and 2036 land uses, longer climate changes increased all N components (i.e., long-term > mid-term > short-term > baseline climate) (Tables 4 and 5). Under the baseline climate, N and P leaching for 1976 land use were maximized, followed by 2006 and 2036. Within each climate scenario, leaching of both elements for 2036 land use tended to be less than those for 2006. Table 6 lists seasonal change in monthly yield of total N under different scenarios in the entire watershed. The decreased magnitude of N from climate change in April and October was greater than that in other months. On the other hands, monthly N yield in March increased by climate change both in 2006 and 2036 land uses (Table 6). As a result, climate change caused the snowmelt peak of N yield to be earlier (March) relative to the baseline climate (April), for each land-use scenario (Table 6).

4. Discussion

4.1. Impact of land-use on water quality

Under the baseline climate, total N and P loads for 1976 land use were greater than those for 2006 and 2036 land uses, suggesting that greater fertilizer input in 1976 contributed to increased nitrate leaching from soil to river (Tables 4 and 5). It is also suggested that higher water yields in the snowmelt (April) and rainy (October) seasons enhanced nutrient loads (especially N) during these period (Fig. 3,Tables 4 and 6). Applied nitrogen (as fertilizer) not taken up by crops becomes a potential source for losses via ammonia volatilization and denitrification to the atmosphere and leaching to aquatic systems (Cassman et al., 2002). Although the fertilizer amount for 2036 land use is higher than that for 2006 (Tables 4 and 5) because of a shift from paddy field to farmland (Fig 2), total N and P yields for 2036 land use were less than those for 2006 land use (Table 3). This suggested that complex factors, including higher crop nutrient uptake, less nitrate leaching, and reduced mineralization of organic matter by land-use change contributed to those nutrient yield changes (Tables 4 and 5). Monthly nitrogen uptake from May through August (the period of fertilizer application,

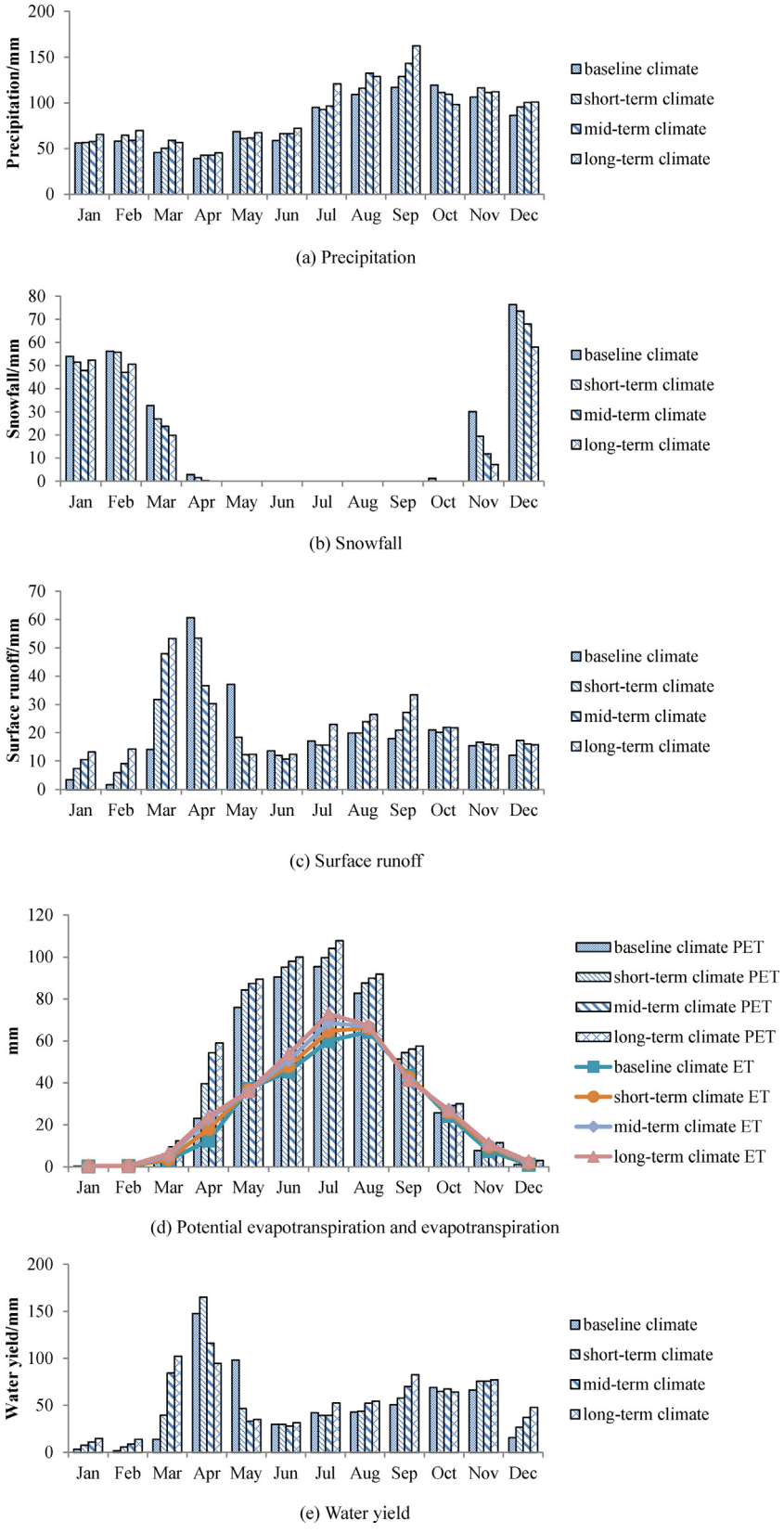

Fig. 5. Water-balance components under climate change scenarios and 2006 land use.

without snow cover) for 2036 land use was greater than that for 2006 land use (Annex, Table A-4), which contributed to a decrease of N yield during this period (Table 6).

Nutrient loads, especially organic forms, are often correlated with sediment transport rates, because both yields are closely related to surface soil erosion (Marshall and Randhir, 2008). In the

Table 2
Average annual hydrologic components and water quantity under scenarios in entire watershed (mm year^{-1}).

Scenarios		Components				
Land use	Climate	Surface runoff	Lateral flow	Groundwater	Evapotranspiration	Water yield
1976	Base	227.5	238.1	120.5	303.6	574.8
2006	Base	234.2	228.3	130.7	298.7	581.8
	Short	239.5	237.3	138.4	317.0	603.3
	Mid	248.0	246.1	141.6	330.9	623.3
	Long	271.8	259.2	153.4	342.0	671.2
2036	Base	238.1	237.4	113.7	300.1	577.8
	Short	244.2	246.6	121.6	317.4	600.3
	Mid	252.9	255.7	125.4	330.5	621.6
	Long	277.2	269.3	136.9	341.0	670.2

The 1976, 2006 and 2036 designators in the scenarios mean land-use scenarios in 1976 (observed), 2006 (observed) and 2036 (predicted), respectively. The Base, Short, Mid and Long designators in the scenarios mean climate changes in baseline (observed for 1976–2009), short-term prediction (2010–2039), mid-term prediction (2040–2069) and long-term prediction (2070–2099), respectively.

Table 3
Average annual yields of sediment, nitrogen (N) and phosphorus (P) under multiple land-use and climate change scenarios in entire watershed of Teshio River.

Scenarios		Components						
Land use	Climate	Sediment (t ha^{-1})	Total N (kg N ha^{-1})	Total P (kg P ha^{-1})	Organic-N (kg N ha^{-1})	Inorganic-N (kg N ha^{-1})	Organic-P (kg P ha^{-1})	Inorganic-P (kg P ha^{-1})
1976	Base	0.052	6.98	0.45	1.09	5.89	0.29	0.16
2006	Base	0.061	6.11	0.31	0.52	5.68	0.23	0.079
	Short	0.072	6.64	0.41	0.68	5.97	0.30	0.11
	Mid	0.081	7.27	0.46	0.78	6.49	0.34	0.12
	Long	0.087	8.58	0.50	1.40	7.19	0.38	0.13
2036	Base	0.041	5.85	0.25	0.67	5.18	0.18	0.066
	Short	0.053	6.35	0.32	0.88	5.46	0.24	0.085
	Mid	0.061	7.09	0.37	1.02	5.97	0.27	0.099
	Long	0.066	7.75	0.41	1.12	6.63	0.30	0.11

Abbreviations for land-use and climate change scenarios are the same as in Table 2.

Table 4
Average annual nitrogen components under multiple land-use and climate change scenarios in entire watershed of Teshio River (kg N ha^{-1} year^{-1}).

Scenarios		Components					
Land use	Climate	Fertilizer	Deposition	Uptake	Denitrification	Leaching	Mineralization
1976	Base	30.7	5.78	56.2	36.7	16.5	68.1
2006	Base	24.3	5.78	52.2	34.0	14.9	67.3
	Short	24.3	6.00	56.8	36.3	15.6	73.8
	Mid	24.3	6.21	59.7	37.6	17.4	79.0
	Long	24.3	6.58	61.8	38.8	18.9	82.8
2036	Base	25.7	5.78	53.7	33.3	13.7	66.7
	Short	25.7	6.00	58.3	35.6	14.5	73.1
	Mid	25.7	6.21	61.3	36.7	16.3	78.3
	Long	25.7	6.58	63.4	37.8	17.8	82.1

Abbreviations for land-use and climate change scenarios are the same as in Table 2. Deposition means atmospheric deposition. Uptake means nutrient uptake by crops.

present study, the sediment load was mainly in April and May and the load in April for 2036 land use was less than that for the 2006 land use. This suggested that the decrease of sediment yield owing to change of hydrologic processes contributed to the decrease of organic N and P yields due to the future land use change (Annex, Tables A-5 and A-6). It is known that hydrologic processes also influence inorganic N leaching from soil to groundwater and river water (Qiu et al., 2011). Our results indicated that groundwater for 2036 land use was less than that for 2006 land use in each climate condition. This suggested that the hydrologic change of the former caused less nutrient leaching than that of the latter (Tables 2 and 4).

In this study, we assumed that driving factors of land use dynamics are constant between past and future due to the data unavailability. However, usual land use transition, especially, agriculture expansion is derived from more complicated driving forces (e.g., decision-maker' behavior), which is difficult for the CLUE model to account for. The agent-based model including decision-making of land management process would be possible to predict such complicated dynamics in agricultural land for the next research step (Luo et al., 2010).

4.2. Impact of climate changes on water quality

Climate changes caused that the nitrogen uptake by plant increased from March to July and decreased in August and September (Annex, Table A-4). Especially, the nitrogen uptake in May was about two times higher under long-term climate changes

Table 5
Average annual phosphorus components under multiple land-use and climate change scenarios in the entire watershed of Teshio River (kg P ha^{-1} year^{-1}).

Scenarios		Components			
Land use	Climate	Fertilizer	Uptake	Leaching	Mineralization
1976	Base	35.6	32.2	0.133	11.7
2006	Base	28.2	31.3	0.126	11.5
	Short	28.2	31.4	0.131	12.6
	Mid	28.2	31.8	0.134	13.5
	Long	28.2	32.1	0.142	14.2
2036	Base	30.5	36.4	0.100	11.4
	Short	30.5	36.8	0.104	12.5
	Mid	30.5	37.2	0.105	13.4
	Long	30.5	37.5	0.112	14.1

Abbreviations for land-use and climate change scenarios are the same as in Table 2.

than that under the baseline climate conditions (Annex, Table A-4). These suggested that the climate changes shifted plant growth earlier due to the higher temperature and ET (Annex, Fig. A-1). The excess applied fertilizers (not absorbed by crops) in the August and September could be potential source of N which was flushed into the stream. It suggested that the higher N uptake in May with lower water yield also contributed to decreased N yield during this period due to the climate changes (Annex, Table A-4; Fig. 5e). These results also suggested that farmers could adequately shift the fertilizer application regimes from the beginning of the planting period (May in this study) to the most active growing period (July in this study) to promote nutrient uptake efficiency with less N leaching potential.

Climate changes also shifted the snowmelt peak from April to March (Fig 5e), suggesting that higher snowmelt increased the monthly N yield in March compared to the base line climate (Table 6). It also indicated that the increased magnitude of nutrient yield in March was larger than decreased magnitude of nutrient yield in April according to the altered magnitude of water yield in March and April. Increased surface runoff in September (rainy season) increased the nutrient loads (Fig. 5, Table 6; Annex, Table A-5). In contrast, a decrease of precipitation in October due to the climate change (Fig. 5a) reduced N yields during that period (Table 6). It suggested the flushing of N by increased water yield in prior month (September) due to climate change (Fig. 5e) also reduced the N potential yield in October (Table 6). The increased temperature also caused a longer period without snow cover, via a decrease of snowfall in November and December and an increase of rainfall (Fig. 5b). These resulted in great increases of monthly nutrient load, because of higher surface runoff in November and December (Table 6; Annex, Table A-5).

Table 6
Monthly change of total nitrogen yield under different scenarios in the entire watershed, units kg N ha^{-1} month^{-1}.

Month	Scenarios								
	1976B	2006B	2006S	2006M	2006L	2036B	2036S	2036M	2036L
1	0.01	0	0.01	0.05	0.17	0	0.02	0.05	0.15
2	0	0	0.01	0.02	0.09	0	0.02	0.03	0.07
3	0.21	0.16	1.60	4.72	5.64	0.17	1.70	4.92	5.66
4	6.19	4.98	4.29	1.66	1.29	5.08	4.43	1.74	1.21
5	1.06	0.83	0.33	0.32	0.40	0.84	0.33	0.31	0.37
6	0.45	0.43	0.47	0.44	0.45	0.41	0.45	0.41	0.42
7	1.08	1.13	0.94	0.91	1.16	1.01	0.84	0.82	1.04
8	0.44	0.47	0.43	0.54	0.50	0.40	0.36	0.46	0.41
9	1.53	1.56	1.66	2.03	2.41	1.30	1.39	1.74	2.10
10	4.12	3.75	3.22	3.15	2.78	3.35	2.88	2.89	2.57
11	5.02	4.50	5.25	5.41	5.65	4.21	4.92	5.13	5.36
12	0.06	0.03	0.44	1.33	2.29	0.04	0.43	1.29	2.18

The 1976, 2006 and 2036 designators in the scenarios mean land-use scenarios in 1976 (observed), 2006 (observed) and 2036 (predicted), respectively. The B, S M and L designators in the scenarios mean climate changes in baseline (observed for 1976–2009), short-term prediction (2010–2039), mid-term prediction (2040–2069) and long-term prediction (2070–2099), respectively.

The timing of sediment yield shifted from April and May under the baseline climate to March and April under future climate changes (Annex, Table A-6). It suggested that the increase of sediment yield in November and December under the long-term climate scenario generated high yields of N and P as organic forms (Annex, Table A-5). Consequently, nutrient loads in March, September, November and December had greater percentages of total annual nutrient loads under climate change scenarios. On the annual scale, the greater increase of temperature accelerated nutrient leaching and mineralization processes (Tables 4 and 5). The increase in hydrologic components, sediment load, nutrient leaching, and mineralization processes were the main drivers of nutrient load amplification, under multiple climate change scenarios.

4.3. Watershed-based mitigation options

Agricultural land contributed more nutrient and sediment loads than other land use under all climate change scenarios (Annex, Figs. A-1 through A-4). In this section, we discussed possible mitigation strategies to reduce the nutrient and sediment loads from watershed. One is establishing riparian zones to buffer nutrient and sediment loads from agricultural land, and the other one is nutrient management strategies (changing the timing and amount of fertilizer) to improve nutrient use efficiency.

The increase of riparian zones along all streams can be possible mitigation option to buffer contaminants entering via surface runoff from farmland and ameliorate water quality impacts resulting from increased fertilizer application (Johnes and Heathwaite, 1997; Webber et al., 2010 Lal et al. 2011). Since riparian zones are prominently located between terrestrial and aquatic ecosystems, riparian processing of nutrients is very effective despite occupying a small area of land relative to the entire catchment. To test the roles of riparian zone to reduce the nutrient and sediment yields, we supplementary simulated the changes of water quality by setting the filter strips in the all agricultural land as a riparian buffer along stream for future land-use, suggesting that the nutrient and sediment loads decreased after establishing riparian zones for all climate scenarios (Annex, Table A-7).

During the fertilizer application period, nitrogen uptake in May alone dramatically increased under future climate change scenarios. The increase in June and July was not as great, and it decreased in August relative to the baseline climate (Annex, Table A-4). Nitrogen not absorbed by crops was potential source that was flushed into streams during the rainy season and snowmelt. The optimum use of nutrients with minimizing nutrient loss and maintaining yield should be planned for the agricultural land management by considering the appropriate fertilizer practices including the choice of adequate chemical form, input rate, application timing, and recycling of crop residues. Modification of amount and timing of fertilizer application would further improve nutrient use efficiency, as would increase amounts used at the beginning, middle and latter of the growing season (May July and August, respectively, in this study). To test the availability of this mitigation option, we supplementarily simulated the water quality with improved fertilizer amount and timing for the future land use with all climate change scenarios, suggesting that the improvement of the fertilizer application decreased the yields of the inorganic N and P in Teshio watershed (Annex, Table A-7). Both the

establishing riparian zones and improved fertilizer application could reduce sediment and nutrient loads from the agricultural land. Especially the riparian zones effectively reduced yields of sediments and dissolved nutrients both could be pollution sources at high concentration in aquatic ecosystem (Annex Table A-7).

To develop sound management schemes for protecting watersheds and to determine the impact of land-use and climate change scenarios on water quantity and quality, our hydrology model was used to simulate nine different land-use and climate change scenarios. Sediment and nutrient loads were mainly from agricultural land under those scenarios. Therefore, we strongly recommend planning of mitigation strategies such as riparian zones, and nutrient management to reduce potentially deleterious impacts of land-use and climate changes.

5. Conclusion

This study provided a framework that integrated future land-use and climate change scenarios to catchment-scale hydrology models to simulate and assess water quantity and quality. We analyzed the impact of land-use and climate changes on hydrology and water quality in the Teshio River watershed of northern Japan. Our major findings are: (i) the climate changes increased surface runoff, lateral flow and groundwater due to increase in precipitation. The climate changes also increased total N and P yields due to altered hydrological process, fertilizer application and nutrient cycle. Those changes are more strongly than land use changes. (ii) There were strong relationships between hydrologic processes, and fertilizer application and water quality under multiple climate change scenarios, especially via shifting peaks of water, sediment and nutrient yields during the snowmelt and rainy periods. (iii) Loads of N, P and sediment were mainly derived from agricultural land under all land-use and climate change scenarios. The establishment of riparian zones and increase of nutrient efficiency by improved fertilizer application were suggested as possible mitigation options to reduce the nutrient loss from agricultural land under the impacts of land-use and climate changes.

Acknowledgments

This study was partly supported by a scholarship from the China Scholarship Council. The work was conducted under the Program for Risk Information on Climate Change, supported by the Ministry of Education, Culture, Sports, Science and Technology of Japan (MEXT).

Appendix A. Supplementary data

Supplementary data associated with this article can be found, in the online version, at http://dx.doi.org/10.1016/j.ecolind.2014.11.003.

References

Alibuyog, N.R., Ella, V.B., Reyes, M.R., Srinivasan, R., Heatwole, C., Dillaha, T., 2009. Prediction the effects of land use change on runoff and sediment yield in Manupali River dubwatershed using the SWAT model. Int. Agric. Eng. J. 18, 15–25.

Arnold, J.G., Allen, P.M., 1996. Estimating hydrologic budgets for three Illinois watersheds. J. Hydrol. 176, 57–77.

Band, L., Mackay, D., Creed, I., Semkin, R., Jeffries, D., 1996. Ecosystem processes at the watershed scale: sensitivity to potential climate change. Limnol. Ocenogr. 41 (5), 928–938.

Bouraoui, F., Galbiati, L., Bidoglio, G., 2002. Climate change impacts on nutrients loads in the Yorkshire Ouse catchment (UK). Hydrol. Earth Syst. Sci. 6 (2), 197–209.

Bouraoui, F., Grizzetti, B., Grandlund, K., Rekolainen, S., Bidodlio, G., 2004. Impact of climate change on the water cycle and nutrient losses in a Finnish catchment. Clim. Change 66, 109–126.

Bradshaw, C.J.A., Sodhi, N.S., Peh, K.S.H., Brook, B.W., 2007. Global evidence that deforestation amplifies flood risk and severity in the developing world. Glob. Change Biol. 13, 1–17.

Bu, H.M., Meng, W., Zhang, Y., Wan, J., 2014. Relationships between land use patterns and water quality in the Taizi River basin, China. Ecol. Indic. 41, 187–197.

Cassman, K.G., Dobermann, A., Walters, D.T., 2002. Agroecosystems, nitrogen-use efficiency, and nitrogen management. AMBIO 31 (2), 132–139.

Chang, H., Evans, B., Easterling, D., 2001. Effects of climate on stream flow and nutrient loading. J. Am. Water Resour. Assoc. 37 (4), 973–986.

Chiang, L., Chaubey, I., Gitau, M.W., Arnold, J.G., 2010. Differentiating impacts of land use changes from pasture management in a CEAP watershed using SWAT model. Trans. ASABE 53, 1569–1584.

Chiang, L.C., Chaubey, I., Hong, N.M., Lin, Y.P., Huang, T., 2012. Implementation of BMP strategies for adaption to climate change and land use change in a pasture-dominated watershed. Int. J. Environ. Res. Public Health 9, 3654–3684.

Chiew, F.H.S., McMahon, T.A., 2002. Modeling the impacts of climate change on Australian streamflow. Hydrol. Process. 23, 486–501.

Fan, M., Shibata, H., 2014a. Water yield, nitrogen and sediment retentions in Northern Japan (Teshio river watershed): land use change scenario analysis. Mitig. Adapt. Strateg. Glob. Change doi:http://dx.doi.org/10.1007/s11027-014-9574-3 (in press).

Fan, M., Shibata, H., 2014b. Spatial and temporal analysis of hydrological provision ecosystem services for watershed conservation planning of water resources. Water Resour. Manage. 28, 3619–3636.

Ferrier, R.C., Whitehead, P.G., Sefton, C., Edwards, A.C., Pugh, K., 1995. Modelling impacts of land use change and climate change on nitrate-nitrogen in the River Don North East Scotland. Water Res. 29 (8), 1950–1956.

Gitau, M.W., Chaubey, I., Gbur, E., Pennington, J.H., Gorham, B., 2010. Impacts of land use change and best management practice implementation in a conservation effects assessment project watershed: Northwest Arkansas. J. Soil Water Conserv. 65, 6353–6368.

Howden, S.M., Soussana, J.F., Tubiello, F.N., Chetri, N., Dunlop, M., Meinke, H., 2007. Adapting agriculture to climate change. Proc. Natl. Acad. Sci. U. S. A. 104, 1961–1969.

Hurkmans, R.T.W.L., Terink, W., Uijlenhoet, R., Moors, E.J., Troch, P.A., Verburg, P.H., 2009. Effects of land use changes on streamflow generation in the Rhine basin. Water Resour. Res. 45, 1–15.

Ileva, N.Y., Shibata, H., Satoh, F., Sasa, K., Ueda, H., 2009. Relationship between the riverine nitrate-nitrogen concentration and land use in the Teshio River watershed, North Japan. Sustainability Sci. 4, 189–198.

IPCC, et al., 2007. Climate Change 2007: Impacts, Adaptation and Vulnerability. Contribution of Working Group II to the Fourth Assessment Report of the Intergovernmental Panel on Climate Change. In: Parry, M.L. (Ed.), Cambridge University Press, Cambridge, UK.

Jeppesen, E., Kronvang, B., Meerhoff, M., et al., 2009. Climate change effects on runoff, catchment phosphorus loading and lake ecological state, and potential adaptations. J. Environ. Qual. 38, 1930–1941.

Jha, M., Pan, Z.T., Takle, E.S., Gu, R., 2004. Impacts of climate change on streamflow in the Upper Mississipi River Basin: a regional climate model perspective. J. Geophys. Res. 109 (D09015) doi:http://dx.doi.org/10.1029/2003JD003686.

Johnes, P.J., Heathwaite, A.L., 1997. Modelling the impact of land use change on water quality in agricultural catchments. Hydrol. Process. 11 (3), 269–286.

Johnson, L.B., Richard, C., Host, G.E., Arthur, J.W., 1997. Landscape influences on water chemistry in Midwestern stream ecosystems. Freshw. Biol. 37 (1), 193–208.

Lal, R., Delgado, J.A., Groffman, P.M., Millar, N., Dell, C., Rotz, A., 2011. Management to mitigate and adapt to climate change. J. Soil Water Conserv. 66 (4), 276–284.

Laurance, W.F., 2007. Forests and floods. Nature 449, 409–410.

Lin, Y.P., Hong, N.M., Wu, P.J., Lin, C.J., 2007. Modeling and assessing land-use and hydrological processes to future land-use and climate change scenario in watershed land-use planning. Environ. Geol. 53, 623–634.

Luo, G., Yin, C., Chen, X., Xu, W., Lu, L., 2010. Combing system dynamic model and CLUE-S model to improve land use scenario analyses at regional scale: a case study of Sangong watershed in Xinjiang, China. Ecol. Complex. 7, 198–207.

Mander, Ü., Meyer, B.C., 2012. Adaptation and functional water management through land use change. Ecol. Indic. 22, 1–3.

Marshall, E., Randhir, T., 2008. Effects of climate change on watershed system: a regional analysis. Clim. Change 89, 263–280.

Manson, S.M., 2005. Agent-based modeling and genetic programming for modeling land change in the Southern Yucatán peninsular region of Mexico. Agric. Ecoyst. Environ. 111, 47–62.

Metzger, M.J., Schröter, D., Leemans, R., Cramer, W., 2008. A spatially explicit and quantitative vulnerability assessment of ecosystem service change in Europe. Reg. Environ. Change 8, 91–107.

Millington, J.D.A., Perry, G.L.W., Calcerrada, R.R., 2007. Regression techniques for examining land use/cover change: a case study of a Mediterranean landscape. Ecosystems 10, 562–578.

Mishima, S., Endo, A., Kohyama, K., 2010. Nitrogen and phosphorus balance on crop production in Japan on national and prefectural scales. Nutr. Cycl. Agroecosyst. 87, 159–173.

Murdoch, P.S., Baron, J.S., Miller, T.L., 2000. Potential effects of climate change on surface water quality in North America. J. Am. Water Resour. Assoc. 36, 347–366.

Nash, J.E., Sutcliffe, J.V., 1970. River flow forecasting through conceptual models. J. Hydrol. 10, 282–290.
Neitsch, S.L., Arnold, J.G., Krniry, J.R., 2011. Soil and Water Assessment Tool Theoretical Documentation Version 2009. Texas Water Resources Institute, College Station, Texas.
Nelson, E., Mendoza, G., Regetz, J., et al., 2009. Modeling multiple ecosystem services, biodiversity conservation, commodity production, and tradeoffs at landscape scales. Front. Ecol. Environ. 7 (1), 4–11.
Noguchi, I., Hayashi, K., Kato, T., Yamaguchi, T., Akiyama, M., Otsuka, H., Sakai, S., Takagi, K., Fukazawa, T., Shibata, H., Fujinuma, Y., Saigusa, N., Shimotori, M., Endo, T., Yago, H., Matsuda, K., Tsunogai, U., Hara, H., 2010. Atmospheric behavior of nitrous acid and nitrogen dioxide in northern Japan. J. Jpn. Soc. Atmos. Environ. 45, 153–165 (in Japanese with English summary).
Pärn, J., Pinary, G., Mander, Ü., 2012. Indicators of nutrients transport from agricultural catchments under temperate climate: a review. Ecol. Indic. 22, 4–15.
Pontius, R.G., Schneider, L.C., 2000. Land use change model validation by a ROC method. Agr. Ecosyst. Environ. 85, 269–280.
Qiu, J.J., Li, H., Wang, L.G., Tang, H.J., Li, C.S., Ranst, E.V., 2011. GIS-model based estimation of nitrogen leaching from croplands of China. Nutr. Cycl. Agroecosyst. 90, 243–252.
Sharpley, A.N., Williams, J.R., 1990. EPIC – erosion productivity impact calculator. 1. Model documentation. U.S. Department of Agriculture, Agricultural Research Service. Technol. Bull. 1768.
Somura, H., Arnold, J., Hoffman, D., Takeda, I., Mori, Y., Luzio, M.D., 2009. Impacts of climate change on the Hii River basin and salinity in Lake Shinji: a case study using the SWAT model and a regression curve. Hydrol. Process. 23, 1887–1900.
Stone, M., Hotchkiss, R., Hubbard, C., Fontaine, T., Arnold, J., 2001. Impacts of climate change on Missouri River Basin water yield. J. Am. Water Resour. Assoc. 37 (5), 1119–1128.
Thampi, S.G., Raneesh, K.Y., Surya, T.V., 2010. Influence of scale on SWAT model calibration for streamflow in a river basin in the humid tropics. Water Resour. Manage. 24, 4567–4578.
Tilman, D., Fargione, J., Wolff, B., et al., 2001. Forecasting agriculturally driven global environmental change. Science 292, 281–284.
Tung, C.P., Lee, T.Y., Yang, Y.C., 2005. Modelling climate-change impacts on stream temperature of Formosan landlocked salmon habitat. Hydrol. Process. 20, 1629–1649.
Turner, M.G., Gardner, R.H., O'Neill, R.V., 2001. Landscape Ecology in Theory and Practice Pattern and Process. Springer-Verlad, New York.
USEPA, 2014. Climate change Site (Online) http://www.epa.gov/climatechange/.
Verburg, P.H., Overmars, K.P., 2009. Combing top-down and bottom-up dynamics in land use modeling: exploring the future of abandoned farmlands in Europe with the Dyna-CLUE model. Landscape Ecol. 24, 1167–1181.
Webber, D.F., Mickelson, S.K., Ahmed, S.I., Russell, J.R., Powers, W.J., Schultz, R.C., Kovar, J.L., 2010. Livestock grazing and vegetation filter strip buffer effects on runoff sediment, nitrate, and phosphorus losses. J. Soil Water Conserv. 65, 34–41.
Williams, J.R., Berndt, H.D., 1977. Sediment yield prediction based on watershed hydrology. Trans. ASAE 20 (6), 1100–1104.
Williams, J.R., Jones, C.A., Dyke, P.T., 1984. A modelling approach to determining the relationship between erosion and soil productivity. Trans. ASAE 27, 129–144.
Williams, T.W.R., Griffiths, J.F., 1995. An assessment of weather generator (WXGEN) used in the erosion/productivity impact calculator (EPIC). Agric. For. Meteorol. 73, 115–133.